Generation of artificial inflow turbulence including scalar fluctuation for LES based on Cholesky decomposition

Tsubasa OKAZE[1], Akashi MOCHIDA[2]

[1] *Tohoku University,* #1205 6-6-11 Aoba, Aramaki Aza, Aoba-ku, Sendai*, 980-8579, Japan,*
okaze@sabine.pln.archi.tohoku.ac.jp
[2] *Tohoku University,* #1202 6-6-11 Aoba, Aramaki Aza, Aoba-ku, Sendai*, 980-8579, Japan,*
mochida@sabine.pln.archi.tohoku.ac.jp

1. Introduction

Most attempts to couple engineering computational fluid dynamics (CFD) models with the mesoscale meteorological model (MMM) have used turbulence models based on Reynolds-averaged Navier-Stokes equations. Recently, increased access to computing power has led to several attempts to couple large-eddy simulation (LES) and MMM. Regarding the coupling of LES with MMM, one of the biggest unresolved issues involves the generation of an inflow turbulence which satisfies not only the turbulent statistics but also the instantaneous turbulent structures. To this end, several techniques have been developed in the fields of wind engineering and building science. These pioneering techniques for generating inflow turbulence within a neutral boundary layer can be classified into two categories. The first, and also the simplest, involves storing the time history of velocity fluctuations obtained from a preliminary or recycling LES computation (Lund et al., 1998; Kataoka and Mizuno, 2002). The second involves artificially generating inflow turbulence which prescribes turbulent statistics without conducting an LES computation (Lee et al., 1992; Iizuka et al., 1999; Klein et al., 2003; Xie and Castro, 2008; Xuan and Iizuka, 2014). In recent years, non-isothermal LES computations within urban boundary layers have been carried out to investigate heat island phenomena and so on. When LES is applied to a non-isothermal field, not only the inflow velocity fluctuation but also the temperature fluctuation should be reproduced. Regarding the generation of inflow turbulence considering temperature fluctuation, only a few studies have been conducted based on the method using the recycling LES mentioned above (Tamura et al., 2012; Jiang et al., 2012) in the wind engineering field.

This paper proposes a new method of generating turbulent fluctuations in wind velocity and scalar quantities such as temperature and contaminant levels based on a Cholesky decomposition of the time-averaged turbulent flux tensors of momentum and scalar. The artificial turbulent fluctuations generated by this method satisfy not only the prescribed profiles for the turbulent fluxes of momentum and scalar but also the prescribed spatial and time correlations. According to the method proposed by Xie and Castro (2008), two-dimensional random data are filtered to generate a set of two-dimensional data with the prescribed spatial correlation. Then, these data are combined with those from the previous time step by using two weighting factors based on an exponential function. The method was validated by applying it to a LES computation of contaminant dispersion in a half-channel flow.

2. New method of generating inflow turbulence including scalar fluctuation

In this study, we express the values of wind velocity and scalar as f_i, the time-averaged values of f_i as $\langle f_i \rangle$, and the deviation from the time-averaged value as f_i':

$$f_i = \langle f_i \rangle + f_i' , \tag{1}$$

where the subscript, i = 1, 2, 3, indicates the wind velocity components in the streamwise, lateral, and vertical directions (u, v, w), respectively, and i = 4 indicates the scalar value ϕ. A regular matrix of the turbulent fluxes of momentum and scalar, R_{ij}, is defined as

$$R_{ij} = \begin{pmatrix} \langle u'u' \rangle & \langle u'v' \rangle & \langle u'w' \rangle & \langle u'\phi' \rangle \\ \langle v'u' \rangle & \langle v'v' \rangle & \langle v'w' \rangle & \langle v'\phi' \rangle \\ \langle w'u' \rangle & \langle w'v' \rangle & \langle w'w' \rangle & \langle w'\phi' \rangle \\ \langle \phi'u' \rangle & \langle \phi'v' \rangle & \langle \phi'w' \rangle & \langle \phi'\phi' \rangle \end{pmatrix} . \tag{2}$$

If the Cholesky decomposition of R_{ij} is implemented, we obtain a lower triangular matrix, a_{ij}, as

$$a_{ij} = \begin{pmatrix} \sqrt{R_{11}} & 0 & 0 & 0 \\ R_{21}/a_{11} & \sqrt{R_{22} - a_{21}^2} & 0 & 0 \\ R_{31}/a_{11} & R_{32} - a_{21}a_{31}/a_{22} & \sqrt{R_{33} - a_{31}^2 - a_{32}^2} & 0 \\ R_{41}/a_{11} & R_{42} - a_{21}a_{41}/a_{22} & R_{43} - a_{31}a_{41} - a_{32}a_{42}/a_{33} & \sqrt{R_{44} - a_{41}^2 - a_{42}^2 - a_{43}^2} \end{pmatrix} . \tag{3}$$

With the lower triangular matrix, a_{ij} and a variable Ψ_j satisfying $\langle \Psi_j \rangle = 0$ and $\langle \Psi_i \Psi_j \rangle = \delta_{ij}$, the fluctuations, f_i, can be rewritten as

$$f_i = \langle f_i \rangle + f_i' = \langle f_i \rangle + a_{ij} \Psi_j . \tag{4}$$

Here, δ_{ij} is the Kronecker delta. We extended the transformation originally proposed by Lund et al. (1998) using Reynolds stress tensors to consider the turbulent fluxes of scalar. The statistics obtained by using Eq. (4) mathematically satisfy the prescribed turbulent fluxes of momentum and scalar in Eq. (2).

To impose time and space correlations for each component of the fluctuations, the two-dimensional digital-filter method proposed by Xie and Castro (2008) and then revised by Kondo and Iizuka (2012) was employed. The prescribed time and space correlations are assumed using exponential functions with an integral time scale, T, and a length scale, L:

$$\frac{\langle \Psi_j(t)\Psi_j(t+\tau) \rangle}{\langle \Psi_j(t)\Psi_j(t) \rangle} = \exp\left(-\frac{\tau}{T}\right), \tag{5}$$

$$\frac{\langle \Psi_j(r)\Psi_j(r+\lambda) \rangle}{\langle \Psi_j(r)\Psi_j(r) \rangle} = \exp\left(-\frac{\lambda}{L}\right), \tag{6}$$

The time advances of artificially generated fluctuations on a grid point (m, n) are expressed as

$$\Psi_j(t+\Delta t, m, n) = \Psi_j(t,m,n)\exp\left(-\frac{\Delta t}{T}\right) + \psi_j(t+\Delta t, m, n)\left\{1 - \exp\left(-\frac{2\Delta t}{T}\right)\right\}^{\frac{1}{2}}, \tag{7}$$

$$\psi_j(t,m,n) = \sum_{m'=1}^{N_y}\sum_{n'=1}^{N_z} b_{m'} b_{n'} r_{m+m', n+n'}, \tag{8}$$

where r is a random number satisfying $\langle r_j \rangle = 0$ and $\langle r_i r_j \rangle = \delta_{ij}$, N_y and N_z are the number of grid points included in the generated plane in each direction, b_k is a digital-filter coefficient for the integral length scale in the generated plane in each direction. The intervals of convolution operation in Eq. (8) proposed by Kondo and Iizuka (2012) were used in this study. The filter coefficient is defined as

$$b_k = \tilde{b}_k / \left(\sum_{j=1}^{N} \tilde{b}_j^{\,2}\right)^{\frac{1}{2}}, \tag{9}$$

$$\tilde{b}_k = \exp\left(-\frac{\Delta x|k|}{L}\right). \tag{10}$$

By substituting ψ_j (as obtained using a new dataset of random numbers using Eqs. (8) to (10)) into (7) for each time step, Ψ_j for the next time step is obtained. Then, the fluctuations, f_i, are given by substituting Ψ_j into Eq. (4).

3. Outline of LES computations

A priori LES computations for a half-channel were carried out to validate the reproducibility of the flow and dispersion field by applying the artificially generated wind and scalar fluctuations as inflow boundary conditions. Fig. 1 is a schematic of the computations. The computational conditions are summarized in Table 1.

First, a preliminary LES computation was conducted to obtain turbulent statistics. This requires the generation of wind and scalar fluctuations. A periodic boundary condition was imposed in both the streamwise and lateral directions for the wind field. An averaged pressure gradient was imposed in the streamwise direction as a driving
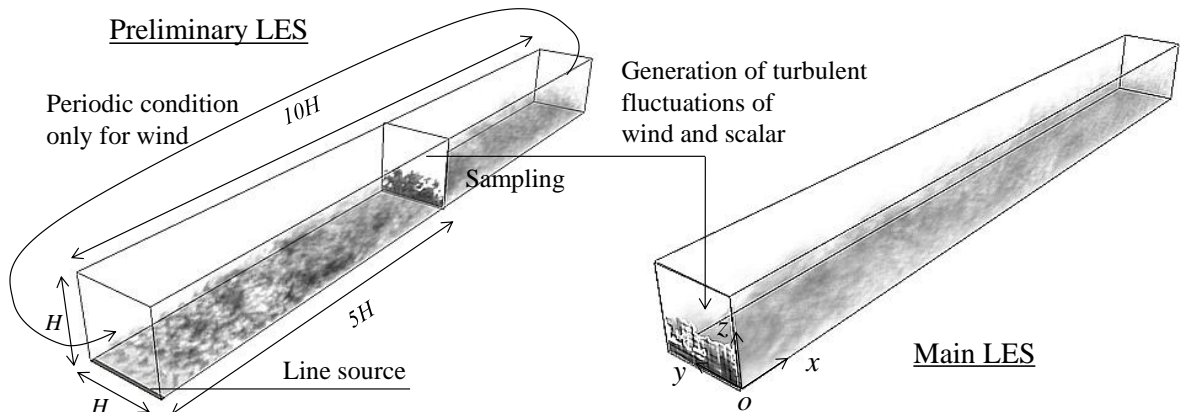
Fig. 1 Schematic view of LES computations

force. The standard Smagorinsky model was applied. For the spatial discretization in the governing equations, a second-order central difference scheme was used. A line source was placed on the ground cell immediately behind the inflow boundary and a passive scalar was emitted. The emission rate of the passive scalar per unit time and unit area was set to 1.0 ($\langle \overline{w'c'} \rangle = 1.0$). The periodic boundary condition was imposed only in the lateral direction of the dispersion field. The time series of the turbulent fluctuations of the wind and scalar values were stored on the y-z plane at $x = 5.0H$. Then, the fluctuations in the wind and scalar values were artificially generated based on the Cholesky decomposition of the time-averaged turbulent flux tensor of momentum and scalar which were obtained from the database collected at $x = 5.0H$ in the preliminary simulation.

Next, the main LES computation was carried out with the artificially generated turbulent fluctuations as the inflow boundary conditions of the main computation. By comparing the results for the flow and the dispersion fields at $x = 1.0H$, $3.0H$, and $5.0H$ in the main calculation with those obtained with $x = 6.0H$, $8.0H$, and $10.0H$ in the preliminary calculation, the reproducibility of the flow and dispersion fields when applying the artificially generated wind and scalar fluctuations as inflow boundary conditions was validated.

The integral length scales for prescribing the space correlations of the turbulent fluctuations of wind velocity were assumed to be $L = 0.15H$, based on the results of a previous study which examined the same situation of a half-channel simulation for investigating the effects of artificially generated fluctuations of the wind velocity components on a reproduced flow field (Kondo and Iizuka, 2012). The integral time scales for prescribing the time correlations of the turbulent fluctuations were given based on the frozen turbulence approximation known as "Taylor's hypothesis":

$$T = L/U ,\qquad\qquad\qquad\qquad (11)$$

where U is the time- and space-averaged wind velocity at the upper boundary. It is assumed that the integral length and time scales for scalar dispersion are equal to those for the wind velocity.

The turbulent statistics for both simulations were collected and averaged over $10\Delta T^*$ after a sufficient initial calculation. The non-dimensional time, ΔT^*, is defined as $\Delta T^* = \Delta T \cdot \langle u^* \rangle / H$, where ΔT is the calculation time, $\langle u^* \rangle$ is the friction velocity on the surface of the ground and H is the domain height.

4. Results and discussion

4.1. Turbulent statistics for generated fluctuations in wind and scalar

Fig. 2 shows a comparison of the turbulent statistics between the targeted values obtained from the preliminary simulation and the artificially generated values based on the method proposed in Chapter 2. The generated mean wind velocity and concentration are in good agreement with the targeted values. The variance of the generated concentration and the turbulent scalar flux in the vertical direction as obtained from the artificial generation are also in good agreement with the targeted values. Thus, we confirmed that the generated turbulent fluctuations in the wind and scalar values, as obtained by this proposed method, satisfy the prescribed time-averaged turbulent flux tensors of momentum and scalar.

4.2. Reproducibility of flow and dispersion fields with artificially generated inflow boundary conditions

Fig. 3 shows the streamwise change in the vertical distributions of the turbulent statistics for the flow field. The mean wind velocity changes very little in the downstream region and is in good agreement with the target value obtained from the preliminary simulation. The turbulent kinetic energy in the grid scale at $x = 1.0H$, just leeward of the inflow boundary, is rapidly damped by 40%, relative to the target value. As previous researchers have pointed out, the causes are suspected to be related to the artificially generated fluctuations not generally being able to satisfy the continuity and momentum equations, while the generated fluctuations database does not include the fluctuations in pressure (Xie and Castro, 2008; Kondo and Iizuka, 2012). The turbulence kinetic energy near the surface more closely approaches the target value as the flow moves downstream, due to the reproduction of the turbulent kinetic energy by the gradient of the mean wind velocity near the surface. In Fig. 3 (3), the variance in the streamwise component of the wind velocity fluctuation decreases by 40% at $x = 1.0H$ and increases as the flow moves downstream. This streamwise change is similar to that of the turbulent kinetic energy. On the other hand, in Fig. 3 (4), the variance in the vertical component of the wind velocity fluctuation falls significantly at $x = 1.0H$, especially near the surface. One of the reasons for this decrease in the vertical component of the wind velocity fluctuation is thought to be that both the integral length scales in the streamwise and vertical directions are set to the same value.

Fig. 4 indicates the streamwise change in the vertical distribution of the mean concentration $\langle \overline{c} \rangle$. The result of the mean concentration obtained from the main simulation with artificially generated fluctuations is slightly larger than the result of the preliminary simulation near the surface. This difference could be attributed to the underestimation of the turbulent diffusion of the passive scalar in the upward direction due to the damping of the turbulent kinetic energy near the inflow boundary.

The streamwise change in the vertical distributions of the turbulent flux of the passive scalar for vertical component $\langle \overline{w'c'} \rangle$ is shown in Fig. 5. The peak values of $\langle \overline{w'c'} \rangle$ for both simulations are observed at the same height in each measured line. However, the turbulent flux at $x = 1.0H$ is somewhat smaller than that due to the underestimation of the turbulent kinetic energy. The flux near the ground surface increases at $x = 3.0H$ and $5.0H$ with an increase in the turbulent kinetic energy near the ground.

Table 1 Computational conditions

Computational domain	$10H(x) \times H(y) \times H(z)$
Grid arrangement	$320(x) \times 32(y) \times 32(z)$
SGS model	Standard Smagorinsky model ($C_s = 0.10$)
Time advance	Second-order Adams-Bashforth scheme
Spatial derivatives	Second-order central difference scheme
Coupling algorithm	SMAC method
Inflow boundary	Preliminary simulation Flow field: Periodic boundary condition Dispersion field: $\langle \bar{c} \rangle = 0$ Main simulation Flow and dispersion field: Artificially generated fluctuations based on the method proposed in Chapter 2
Outflow boundary	Preliminary simulation Flow field: Periodic boundary condition Dispersion field: $\partial \langle \bar{c} \rangle / \partial x = 0$ Main simulation $\partial \langle \bar{u}_i \rangle / \partial x = 0$, $\partial \langle \bar{c} \rangle / \partial x = 0$
Lateral boundaries	Periodic boundary conditions
Upper boundary	Slip boundary condition
Ground surface	Werner and Wengle's approach (1991) was adopted. A linear 1/7 power law distribution of the instantaneous velocity was assumed.
Reynolds number	1.7×10^4 ($\langle u_0 \rangle \times H / \nu$)
Driving force	Average pressure gradient ($\partial \langle \bar{p} \rangle / \partial x = -0.0015 U^2 / H$)
Turbulent Schmidt number	0.5

(1) $\langle u \rangle / U$ (2) $\langle c \rangle \cdot U / q$ (3) $\langle c'^2 \rangle \cdot U^2 / q^2$ (4) $\langle w'c' \rangle / q$
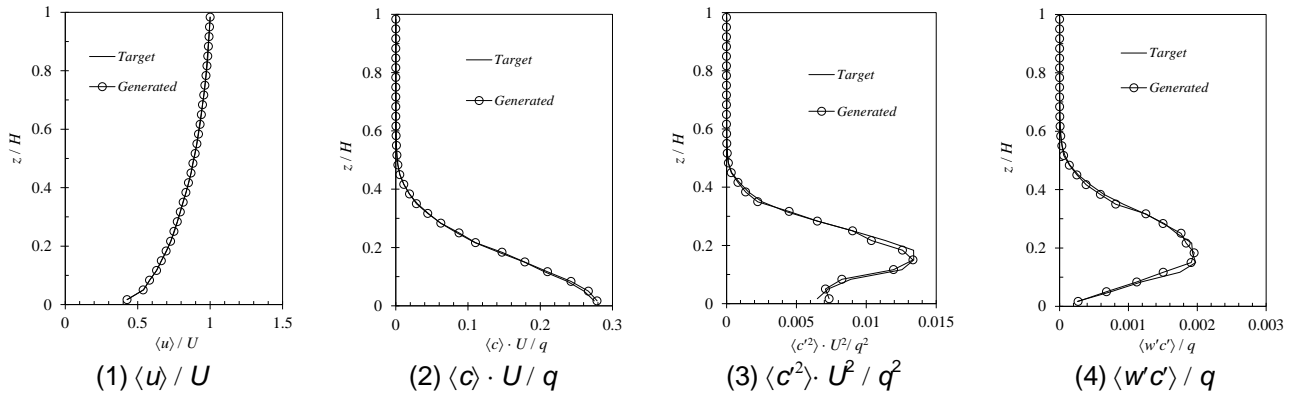
Fig.2 Comparison of turbulent statistics for the targeted values obtained from the preliminary simulation and the artificially generated values based on the proposed method

(1) $\langle \bar{u} \rangle / U$ (2) k / U^2 (3) $\langle \bar{u}'^2 \rangle / U^2$ (4) $\langle \bar{w}'^2 \rangle / U^2$
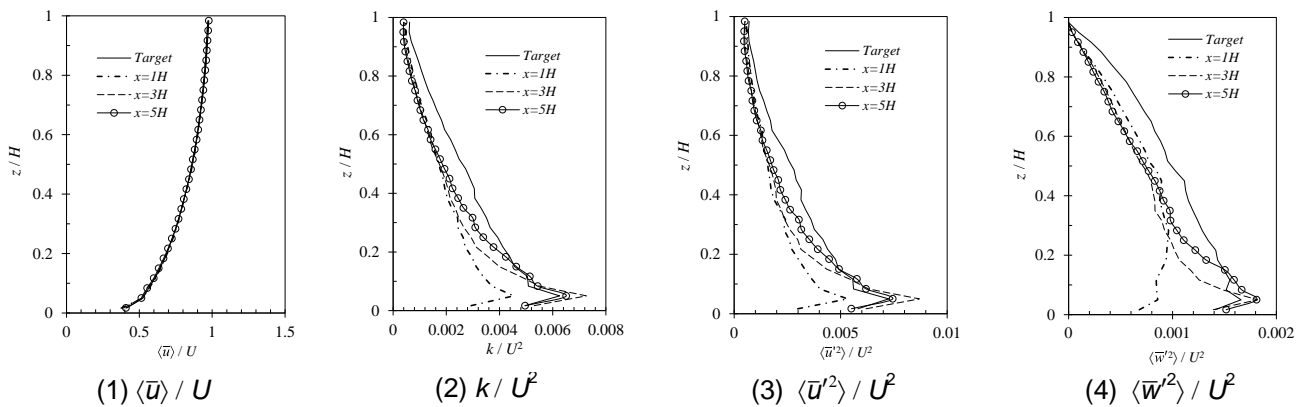
Fig. 3 Streamwise change in vertical distribution in turbulent statistics for flow field

Fig. 6 shows the streamwise change in the vertical distribution of the variance of the passive scalar fluctuation $\langle \overline{c}'^2 \rangle$. The results of the main simulation are overestimated for each line although the distribution profile and the height at which the peak value of $\langle \overline{c}'^2 \rangle$ appears are similar to the results obtained with the preliminary simulation. The underestimation of $\langle \overline{w}'\overline{c}' \rangle$, mentioned above, leads to poor turbulent diffusion, and the high windward concentrations would trend to the leeward side. As a result, $\langle \overline{c}'^2 \rangle$ is overestimated in the main simulation.
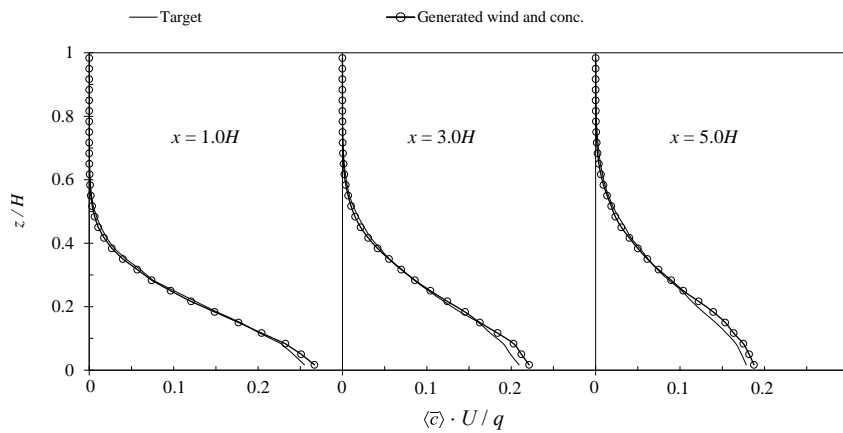
Fig. 4 Streamwise change in vertical distribution of mean concentrations
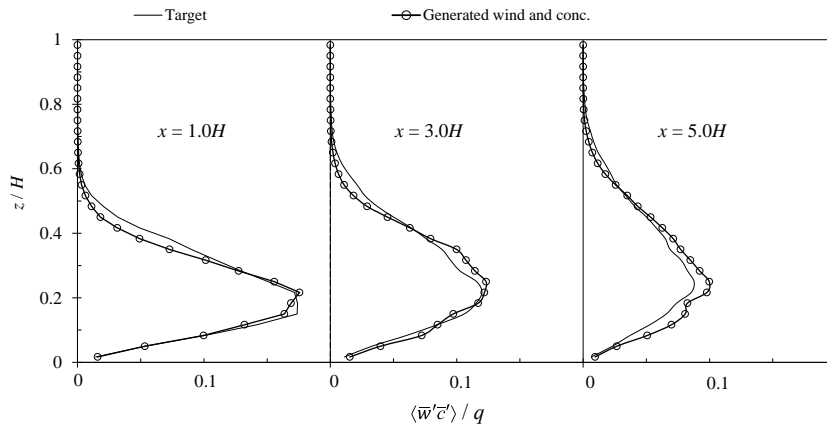
Fig. 5 Streamwise change of vertical distributions of turbulent flux of passive scalar for vertical component
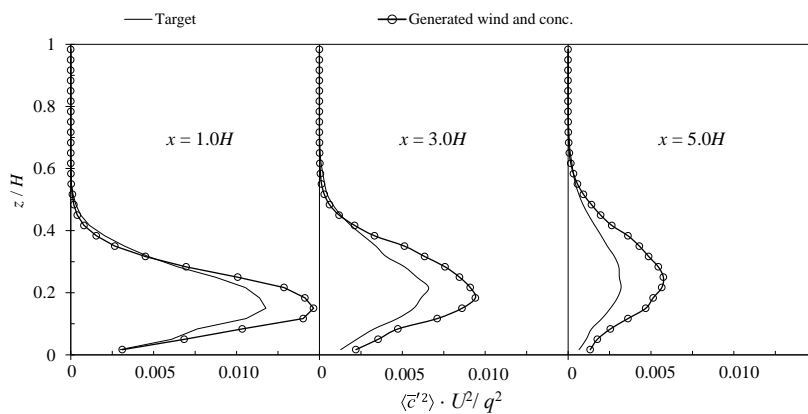
Fig. 6 Streamwise change in vertical distributions of variance of passive scalar fluctuation

4. Conclusions

A new method for generating the turbulent fluctuations in wind velocities and scalar quantities such as temperature and contaminants, based on the Cholesky decomposition of the time-averaged turbulent flux tensors of momentum and scalar, was developed. By employing a 5×5 non-singular matrix as a turbulent flux tensor matrix, the proposed method can generate time series of wind velocity, temperature, and concentration of contaminants and so on. This method can be applied to other artificial generation methods based on the Cholesky decomposition of the Reynolds stresses, including the synthetic eddy method proposed by Jarrin et al. (2006).

LES computations for a half-channel were carried out to validate the reproducibility of the flow and dispersion fields by applying the artificially generated wind and scalar fluctuations as inflow boundary conditions. The streamwise change in the mean concentration was reproduced well by means of a periodic simulation. However, $\langle \overline{w'c'} \rangle$ was underestimated and $\langle \overline{c'^2} \rangle$ was overestimated due to the damping of the turbulent kinetic energy caused by the continuity and momentum balances for the artificially generated wind velocities not being satisfied. Further investigations into the effect of the integral time and length scales on artificially generated fluctuations, as well as the applicability of this method to non-isothermal flow fields should be undertaken.

References

Iizuka S., Murakami S., Tsuchiya N., Mochida A., 1999: LES of flow past 2D cylinder with imposed inflow turbulence. *Proceedings of 10th International Conference on Wind Engineering*, 1291–1298

Jarrin N., Benhamadouche S., Laurence D., Prosser R., 2006: A synthetic-eddy-method for generating inflow conditions for large-eddy simulations. *International Journal of Heat and Fluid Flow*, **27(4)**, 585–593

Jiang G., Yoshie R., Shirasawa T., Jin X. 2012: Inflow turbulence generation for large eddy simulation in non-isothermal boundary layers. *J. Wind Eng. Ind. Aerodyn.*, **104–106**, 369–378

Kataoka H., Mizuno M., 2002: Numerical flow computation around aeroelastic 3D square cylinder using inflow turbulence. *Wind and Structures*, *5*, 379–392

Kondo A., Iizuka S., 2012: An investigation of artificial generation methods of inflow turbulence for LES based on the Cholesky decomposition of Reynolds stresses: Development of a seamless merging method of mesoscale/regional meteorological models and engineering LES models (Part 1). *Transactions of AIJ, Journal of Environmental Engineering*, **77(678)**, 661-669 (in Japanese with English abstract).

Klein M., Sadiki A., Janicka J., 2003: A digital filter based generation of inflow data for spatially developing direct numerical or large eddy simulations. *Journal of Computational Physics*, **186**, 652–665

Lee S., Lele S. K., Moin P., 1992: Simulation of spatially evolving turbulence and the applicability of Taylor's hypothesis in compressible flow, *Physics of Fluids*, **A4**, 1521-1530

Lund T. S., Wu X., Squires K. D., 1998: Generation of turbulent inflow data for spatially-developing boundary layer simulations, *Journal of Computational Physics*, **140(2)**, 233-258

Tamura T., Nozu T., Okuda Y., Ohashi M., Umakawa H., 2012: Hybrid method of meteorological and LES models for heat environment, *USB proceedings of 8th International Conference on Urban Climates*

Xie Z.T., Castro I. P., 2008: Efficient Generation of Inflow Conditions for Large Eddy Simulation of Street-Scale Flows. *Flow, Turbulence and Combustion*, **81(3)**, 449–470

Xuan Y., Iizuka S., 2014: Effects of imposing the continuity condition on artificially generated inflow turbulence for LES. *USB proceedings of 6th international conference on Computational Wind Engineering*